The Meteoritical Society

Meteoritics & Planetary Science 42, Nr 10, 1791–1800 (2007)
Abstract available online at http://meteoritics.org

Global mapping of the degree of space weathering on asteroid 25143 Itokawa by Hayabusa/AMICA observations

Masateru ISHIGURO[1*], Takahiro HIROI[2], David J. THOLEN[3], Sho SASAKI[4], Yuji UEDA[5], Tokuhiro NIMURA[5, 6], Masanao ABE[6], Beth E. CLARK[7], Aya YAMAMOTO[8], Fumi YOSHIDA[9], Ryosuke NAKAMURA[10], Naru HIRATA[11], Hideaki MIYAMOTO[12], Yasuhiro YOKOTA[6], Tatsuaki HASHIMOTO[6], Takashi KUBOTA[6], Akiko M. NAKAMURA[13], Robert W. GASKELL[14, 15], and Jun SAITO[16]

[1]Department of Physics and Astronomy, Seoul National University, Seoul 151-742, Korea
[2]Department of Geological Sciences, Brown University, Providence, Rhode Island 02912, USA
[3]Institute for Astronomy, University of Hawai'i, 2680 Woodlawn Drive, Honolulu, Hawai'i 96822, USA
[4]RISE Project, National Astronomical Observatory of Japan, Mizusawa, Oshu 023-0861, Japan
[5]Department of Earth and Planetary Science, University of Tokyo, Hongo, Bunkyo-ku, Tokyo 113, Japan
[6]Institute of Space and Astronautical Science (ISAS), Japan Aerospace Exploration Agency (JAXA), Sagamihara, Kanagawa 229-8510, Japan
[7]Physics Department, Ithaca College, Ithaca, New York 14850, USA
[8]Remote Sensing Technology Center of Japan (RESTEC), 1-9-9 Roppongi, Tokyo 106-0032, Japan
[9]National Astronomical Observatory of Japan, Mitaka, Tokyo 181-8588, Japan
[10] National Institute of Advanced Industrial Science and Technology (AIST), Tsukuba 305-8568, Japan
[11]Department of Computer Software, University of Aizu, Aizu-wakamatsu, Fukushima 965-8580, Japan
[12]The University Museum, University of Tokyo, Tokyo 113-0033, Japan
[13]Graduate School of Science, Kobe University, 1-1 Rokkodai-cho, Nada-ku, Kobe, 657-8501, Japan
[14]Jet Propulsion Laboratory, California Institute of Technology, Pasadena, California 91109, USA
[15]Planetary Science Institute (PSI), P.O. Box 135 Altadena, California 91003, USA
[16]Satellite Business Division, PASCO Corporation, 2-8-10 Higashiyama, Meguro-ku, Tokyo 153-0043, Japan
[*]Corresponding author. E-mail: ishiguro@astro.snu.ac.kr; ishiguro@planeta.sci.isas.jaxa.jp

(Received 12 October 2006; revision accepted 22 April 2007)

Abstract–We obtained color images of near-Earth asteroid 25143 Itokawa by the Hayabusa multi-band imaging camera to characterize the regional color properties. Images were obtained for the whole disk from the gate position (GP) and home position (HP) at a spatial resolution of 0.8–3.7 m/pixel. Whole-disk spectra are adjusted to the telescopic data obtained by the University of Hawai'i's 88-inch telescope using the Eight Color Asteroid Survey (ECAS) system. The disk-resolved measurements show large variations in the three visible channels. We present a map of an index related to the degree of space weathering, which has been newly developed based on laboratory measurements. We find large variations in the degree of space weathering on Itokawa. Fresh materials are observed in regions of steep slopes and craters, whereas mature materials are ubiquitously distributed. This result suggests that pristine ordinary chondrite-like materials have been exposed through weathered layers by excavation. By also examining close-up images obtained during touchdown rehearsal, we find that most rocks in Itokawa's rough terrains are weathered. Instead of a regolith blanket, the surface of this small asteroid is covered with weathered rocks and gravels.

INTRODUCTION

Remote sensing is an essential approach to learning about the nature of asteroids. Multi-band observations by cameras on board spacecraft provide detailed information regarding chemical and physical properties on the surface of target bodies. As a result of previous asteroid missions, colorimetric studies were reported. Galileo spacecraft images revealed a 5–10% albedo contrast and ~10% color (0.76 μm/0.41 μm) variation on S-type asteroids 951 Gaspra and 243 Ida (Helfenstein et al. 1994; Veverka et al. 1996; Chapman et al. 1996). The color and albedo heterogeneities were correlated

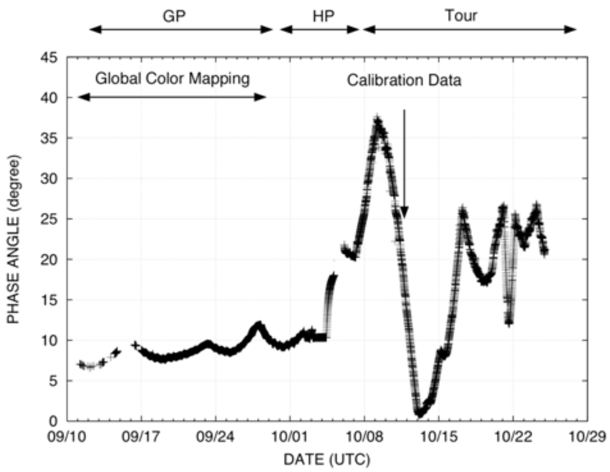

Fig. 1. Phase angle of AMICA boresight. The color data presented in this paper were obtained in the first three weeks at a phase angle of about 10°, while a calibration factor was determined using the data collected on October 11, 2005, at a phase angle of 21°.

with craters, suggesting space weathering processes. Near-Earth object 433 Eros, which was studied by the Near-Earth Asteroid Rendezvous (NEAR) mission, exhibits a large (factor of two) range of albedo, but shows subtle (a few percent at most) color variations (Murchie et al. 2002). It has been suggested that Eros's surface may be completely weathered by a process different from the weathering mechanism on Gaspra and Ida (Clark et al. 2001; Chapman et al. 2002). Since these three S-type asteroids explored by spacecraft are larger than 10 km in diameter, it is particularly interesting to obtain a color map on a sub-kilometer-sized asteroid like Itokawa.

Hayabusa spacecraft successfully rendezvoused with the target asteroid 25143 Itokawa on September 12, 2005, (Fujiwara et al. 2006). For nearly three months, from the end of August (approaching phase) through the end of November (sampling phase), remote-sensing observations were acquired using onboard devices, i.e., two-dimensional cameras, the near-infrared spectrometer (NIRS), the X-ray spectrometer (XRS), the light detection and ranging instruments (LIDAR), and other engineering devices. The initial reports from each instrument team have appeared in Saito et al. (2006), Abe et al. (2006a), Okada et al. (2006) and Abe et al. (2006b); the list of tentative nomenclature on Itokawa is given in Demura et al. (2006). From ground-based observations, Itokawa is categorized as an S(IV)-type or Q-type asteroid, which is thought to be similar to ordinary chondrite meteorites (Binzel et al. 2001; see also Dermawan et al. 2002; Ishiguro et al. 2003; Lowry et al. 2005; Lederer et al. 2005; Cellino et al. 2005). The size (535 × 294 × 209 m), rotational spin (retrograde pole with the rotational period of ~12.132 h) and mass density (1.9 g cm^{-3}), which was determined by the Hayabusa observations (Fujiwara et al. 2006; Abe et al. 2006b), are in good agreement with the values predicted from the ground-based observations (Kaasalainen et al. 2003; Ostro et al. 2004; see also Ohba et al. 2003; Müller et al. 2005; Sekiguchi et al. 2003).

In this paper, we create a color map of Itokawa using the three visible channels. Based on laboratory measurements to simulate space weathering, we develop and map an index related to the degree of space weathering. We then compare the map with the surface morphology in close-up images (spatial resolution of ~1 cm) as well as lower-resolution images, and discuss a potential scenario to explain the variation on Itokawa.

AMICA MULTI-BAND OBSERVATIONS AND THE COLOR MAP OF ITOKAWA

One of the optical navigation cameras (ONC-T) was developed to acquire scientific data as well as for engineering purposes (Nakamura et al. 2001). The Asteroid Multiband Imaging Camera (AMICA) is equipped with a broad-bandpass filter and seven narrow band filters. The narrow-band filter system is nearly equivalent to that of the Eight Color Asteroid Survey (ECAS) system (Tedesco et al. 1982; Zellner et al. 1985); that is, the designed effective wavelengths (and the full width of half-maximum) for solar incident light are 0.38 (0.05) μm (ul-band), 0.43 (0.11) μm (b-band), 0.55 (0.07) μm (v-band), 0.70 (0.07) μm (w-band), 0.86 (0.08) μm (x-band), 0.96 (0.08) μm (p-band), and 1.01 (0.07) μm (zs-band), respectively. During the nearly 3-month observation period in approaching phase and mission phase, AMICA took approximately 1400 images of Itokawa at solar phase angles between 0 and 35° (Fig. 1). About 60% of Itokawa images are obtained for the purpose of shape modeling and topography with lossy compression, and about 40% are for photometric studies with lossless compression.

Global mapping was done from a distance of about 20 km in the gate position (GP) and about 7 km in the home position (HP), a region roughly on a line connecting the Earth with the asteroid on the sunward side. The solar phase angle during GP and HP was small (typically 10°). After substantial observations, the spacecraft left the HP and made a tour (Fujiwara et al. 2006) to observe Itokawa at various attitude and solar phase angle (0–35°; see Fig. 1). The data taken during the tour period is useful not only for the topography and scattering properties of Itokawa's surface, but also for the calibration of camera data using the ground-based data because of the limited conditions of the ground-based observations (most telescopic studies were performed at solar phase angles of 15–90° (see e.g., Lederer et al. 2005).

Most of the color mapping data was obtained in GP and HP when the spacecraft was at an altitude of 8–23 km. The 1 × 1 or 2 × 2 pixel binning, which is the combination of the observed flux of adjacent 1 × 1 or 2 × 2 detector in the CCD, were applied according to the total data amount. A total of 37 sets of multi-color observations were scheduled, but v-band images in 9 sets were found to be useless due to an incorrect operation command. We do not show either the calibrated data in the three longer channels (x-, p-, and zs-band), due to the scattered light problem inside the optics, or the shortest wavelength (ul-band), due to the mismatch between the standard ECAS and AMICA filter system. Therefore, in this paper we focus on the data analysis of 28 sets of lossless data in the b-, v-, and w-bands (Table 1).

Because the exposure time of AMICA is controlled electronically without a mechanical shutter, a so-called "smear" component arises from exposure during the frame transfer (Nakamura et al. 2001). To calibrate the images, smear flux is first subtracted from the originals. In some cases, the smear operations were done onboard, while in others we calculated it using the observed flux of Itokawa itself. The obtained data were divided by the preflight flat-field data in order to correct the uneven sensitivity of pixels and vignetting. We confirmed that there was no significant variation (<3%) in the uniformity of sensitivity by monitoring the internal calibration lamp. Irreproducible stripe patterns, which were induced by the electrical interference with the other devices onboard, were manually subtracted by fitting them with a sine series. A Lucy-Richardson image deconvolution algorithm was applied in order to restore the blurred images (Richardson 1972; Lucy 1974). Point-spread functions for image restoration were characterized using the stellar data obtained in cruising and mission phases. Flux calibration was performed using ground-based photometric data of Itokawa obtained by the University of Hawai'i's 88-inch telescope with the ECAS filter set on February 28, 2001 (phase angle of 21°). We applied a conversion factor to the reflectance from the AMICA b-, v-, and w-band data to adjust the disk-integrated flux of Itokawa to a phase angle of 21° in order to match the ground-based data.

Using calibrated data observed at solar phase angles of 7–11°, we created a false-color map indicating the ratio of the w-band intensity to the b-band intensity (Fig. 2). The map clearly shows that the surface of Itokawa is characterized by two distinct terrains: a bright blue terrain and a dark red terrain. The color and albedo relationship on Itokawa is more similar to that on Gaspra and Ida than that on Eros, but the contrasts of both color and albedo on Itokawa are much sharper than those on Ida and Gaspra.

By analogy to the Moon, blue terrains are thought to be composed of fresher materials, whereas red terrains are mature. However, it is important to note that the color and albedo variations are subject to other effects, such as differences in the composition, variation in grain size (Hiroi and Pieters 1994), viewing geometry (i.e., incident, emergence, and phase angles) (Murchie et al. 2002) and surface roughness (Sakai and Nakamura 2005). It is unlikely that the color and albedo variations are caused by the differences in the composition because of the lack of spatial variations in X-ray fluorescence and the near-infrared spectrometry observations (Abe et al. 2006a; Okada et al. 2006; Hiroi et al. 2006b). It is found that R_w/R_b color ratio is largely independent of incident and emergence angle. In Fig. 3, we show the emergence angle dependence of R_w/R_b color ratio in four terrains, which show negligible change up to ~60°. We can ignore the phase reddening (reddening with increasing phase angles) because the data presented here were taken at narrow-phase angle range (Fig. 1). Accordingly, space weathering is possibly a process that can explain the color and albedo variation on Itokawa.

Table 1. Images used for this study.

Date	b-band	v-band	w-band
2005/9/11	ST_2367901002	ST_2367939436	ST_2367977869
2005/9/12	ST_2370315564	ST_2370353993	ST_2370392422
	ST_2370516209	ST_2370554637	ST_2370593050
	ST_2370977000	ST_2371015429	ST_2371053842
2005/9/17	ST_2385559680	ST_2385578902	ST_2385598109
2005/9/18	ST_2388017311	ST_2388036566	ST_2388055805
2005/9/19	ST_2390417026	ST_2390436248	ST_2390455454
2005/9/21	ST_2395788944	ST_2395794877	ST_2395806303
	ST_2395846546	ST_2395852463	ST_2395863905
2005/9/22	ST_2399076073	–	ST_2399104923
	ST_2399133675	–	ST_2399162524
	ST_2399191276	–	ST_2399220126
	ST_2399248878	–	ST_2399277776
	ST_2399306496	–	ST_2399335378
	ST_2399364097	–	ST_2399392979
	ST_2399421698	–	ST_2399450580
	ST_2399479299	–	ST_2399508165
	ST_2399536901	–	ST_2399565767
2005/9/23	ST_2400804147	ST_2400810032	ST_2400829139
	ST_2400861749	ST_2400867634	ST_2400886741
	ST_2400919351	ST_2400925219	ST_2400944343
	ST_2400976952	ST_2400982820	ST_2401001944
	ST_2401264943	ST_2401270827	ST_2401289935
	ST_2401322545	ST_2401328429	ST_2401347537
	ST_2401380147	ST_2401386031	ST_2401405139
2005/9/24	ST_2403856989	ST_2403862874	ST_2403876261
	ST_2403914592	ST_2403920476	ST_2403933863
	ST_2403972177	ST_2403978078	ST_2403991465
	ST_2404029779	ST_2404035679	ST_2404049066
	ST_2404087380	ST_2404093281	ST_2404106668
	ST_2404836207	ST_2404842124	ST_2404855479
	ST_2404893809	ST_2404899726	ST_2404913081
	ST_2404951411	ST_2404957328	ST_2404970683
	ST_2405009013	ST_2405014930	ST_2405028284
2005/9/25	ST_2406717897	ST_2406727508	ST_2406737168
	ST_2407409109	ST_2407418769	ST_2407428397
2005/9/29	ST_2418659460	ST_2418699769	ST_2418768895
2005/10/11	ST_2450510529	ST_2450514369	ST_2450518275
2005/11/12		ST_2544579522	
		ST_2544617921	

LABORATORY MEASUREMENTS

Itokawa's surface has an olivine-rich mineral assemblage and is potentially related to LL5 or LL6 chondrite materials (Abe et al. 2006a; Hiroi et al. 2006b). We thus focus on LL chondrites here. A broad comparative study of space-weathering indices with other materials is beyond the scope of this application, but will be discussed elsewhere. Harleton

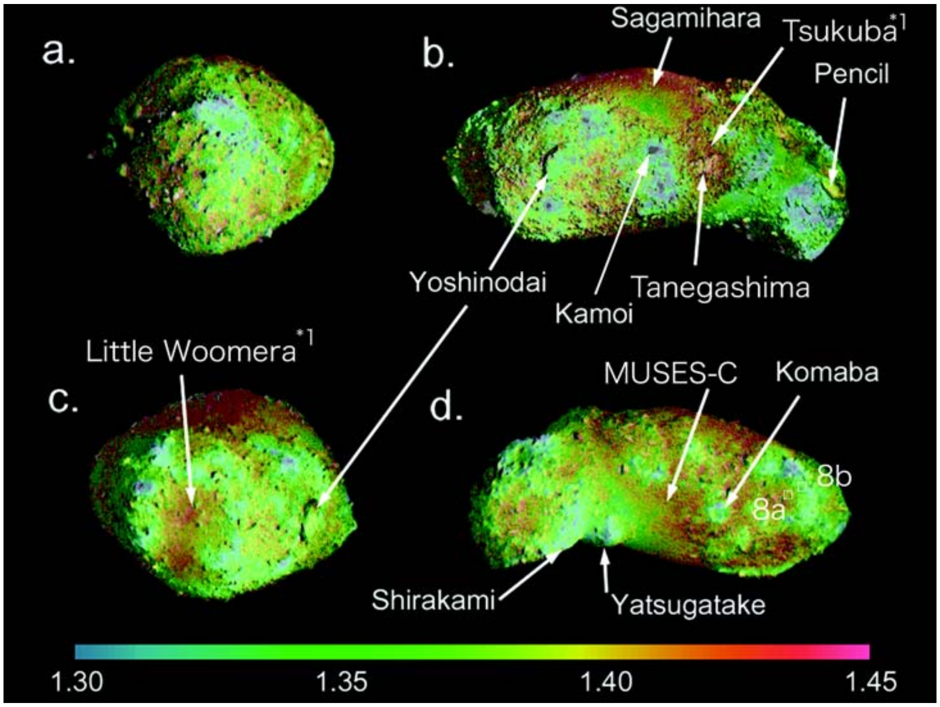

Fig. 2. False-color images of each hemisphere. Intensity is modulated by an underlying w-band image, and R_w/R_b ratio is shown in false color as hue (ST_2385559680-ST_2385598109, ST_2406717897-ST2406737168, ST_2407409109-ST2407428397, ST_2418659460-ST2418768895). The two boxes called "8a" and "8b" are the corresponding areas in Fig. 8.
*Note that Little Woomera and Tsukuba are not formal nomenclature, but tentative names used in previous papers.

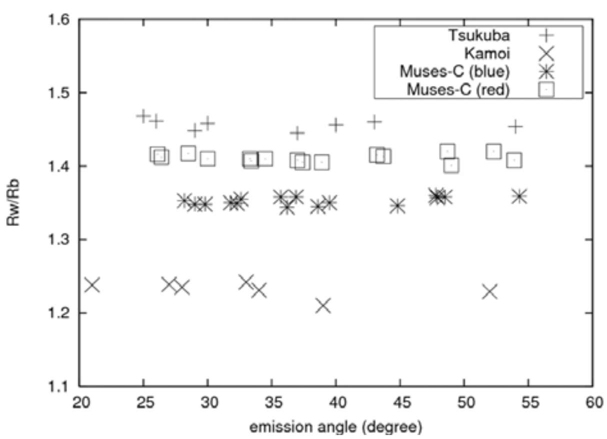

Fig. 3. Emission angle dependences of color ratio (R_w/R_b) in Kamoi crater (bluest crater), Tsukuba basin (one of the reddest regions), and the bluer (Yatsugatake side) and redder parts (in the seashore) of MUSES-C Regio.

(L6) and Cherokee Springs (LL6) ordinary chondrites were prepared in different forms, that is, a chip and powder-size fractions (125–500 and <125 μm). An Alta'ameem (LL5) sample was prepared into a <125 μm size fraction, and powder samples (<250 μm) of Northwest Africa (NWA) 1799 (LL5) were prepared and pressed into pellets. The pellets were irradiated with a pulsed laser at 5 and 15 mJ as a space-weathering simulation (Sasaki et al. 2001) at National Astronomical Observatory of Japan. Bidirectional reflectance spectra of the meteorite samples were taken at various incidence and emergence angles between 0 and 60° at the NASA Reflectance Experiment Laboratory (RELAB) at Brown University, the University of Tokyo, or JAXA/ISAS. It is well known that space weathering strongly alters the visible reflectance spectra of airless planetary surface materials, namely by darkening and reddening (Pieters et al. 1993). It is not as well known that space weathering also causes changes in spectral inflections around 0.42 and 0.55 μm in wavelength. In Fig. 4, we show the normalized reflectance in order to see the change in the inflection. In laboratory experiments, we used a laser beam to simulate the processes of space weathering caused by micrometeorite bombardments. We assume that increasing laser energy corresponds to higher degrees of space weathering (Sasaki et al. 2001). We observe that as the degree of space weathering progresses, inflections at 0.42 and 0.55 μm decrease toward a smoother spectrum. With AMICA multiband spectroscopy, we can quantify the inflections (Hiroi et al. 2006a):

$$C_v = \frac{(1 - R_v/R_w)}{\lambda_w - \lambda_v} - \frac{(R_v/R_w - R_b/R_w)}{\lambda_v - \lambda_b}$$

$$C_b = \frac{(1 - R_b/R_v)}{\lambda_v - \lambda_b} - \frac{(R_b/R_v - R_{ul}/R_v)}{\lambda_b - \lambda_{ul}} \quad (1)$$

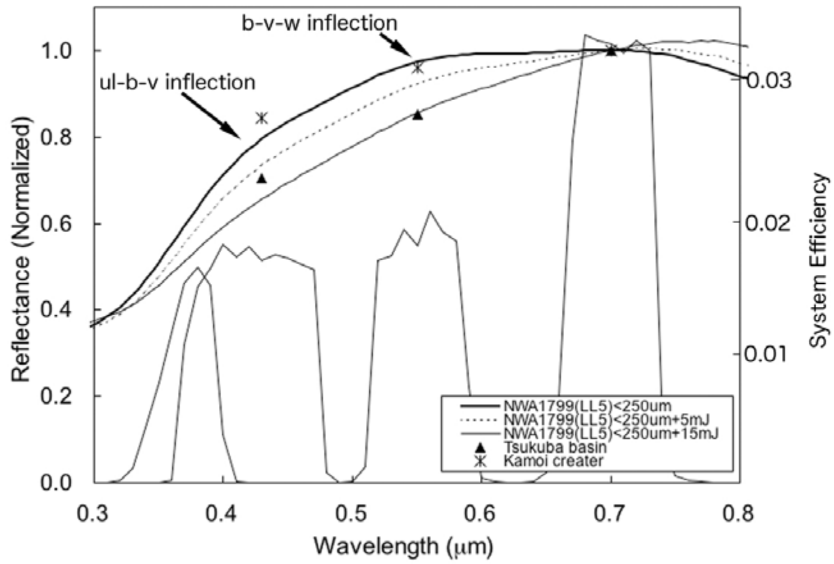

Fig. 4. Plots of visible reflectance spectra of fresh and laser-irradiated LL5 chondrite samples. Example reflectance in Tsukuba basin and Kamoi crater are also plotted. The system efficiencies, which are the predicted throughput performance of the AMICA optical system and CCD quantum efficiency, are drawn for reference.

where R_x and λ_x indicate reflectance and effective wavelength for a band x, respectively.

From our experiments, it is found that 1) both C_v and C_b show a good correlation to the amount of irradiated pulse-laser energy in NWA 1799 LL5 chondrite sample (Fig. 5); 2) C_v and C_b values for the Alta'ameem LL5 sample show negligible change up to 50° of phase angle and up to 60° of incident angle (Figs. 6a and 6b); and 3) C_v for both Cherokee Spring LL6 and Harleton L6 samples is largely independent of the grain size (Fig. 6c; see also Hiroi et al. 2006a). In Figs. 4 and 5, we plot the reflectance and C_v in the fresh-looking Kamoi crater and the matured Tsukuba basin (surrounding area of Tanegashima boulder), two terrains that differ strongly in color properties. (Note that Tsukua is a tentative name used in previous papers; see, e.g., Demura et al. 2006). Both the reflectance and C_v of the bright blue crater Kamoi is similar to that of a fresh ordinary chondrite sample.

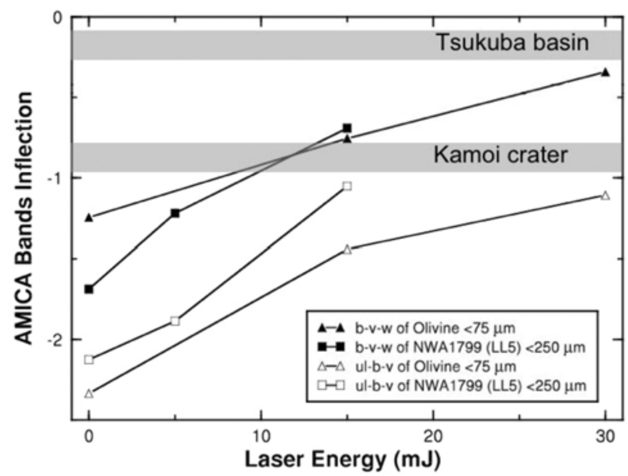

Fig. 5. Correlation between the amounts of ul-b-v-w inflections and the degree of space weathering (indicated by laser energy). C_v (b-v-w inflection) values of Tsukuba basin and Kamoi crater are also shown.

RESULTS

Space Weathering Map

We apply the C_v index to AMICA data; the results are shown in Fig. 7. The boundary of the solar incident angle of 60° is delineated to delimit the effective region of the C_v index by applying Itokawa's shape model (Gaskell et al. 2006). Most fresher (bluer) areas in Fig. 7 correspond with brighter and bluer regions in Fig. 2. Thus, we could conclude that a plausible explanation for the color and albedo effects observed on Itokawa is space weathering. No significant difference has been observed in space weathering between "head" and "body." The overall degree of freshness is greater for the western (Tsukuba) side than the eastern (MUSES-C Regio) side. This might be related to the difference in general appearances of large boulders; the eastern side has a rougher surface due to larger numbers of big boulders (Fujiwara et al. 2006). While differences in the degree of space weathering are limited between two smooth terrains (MUSES-C Regio and Sagamihara Regio), significant variations are observed in rough (boulder-rich) terrains. Although most rough terrains are weathered, pristine areas are found specifically in regions of steep slopes (e.g., Shirakami region, edge of Little Woomera) and crater rims (e.g., Kamoi crater). In addition, big boulders (e.g., Yoshinodai, Pencil, and Tanegashima boulders) are found to be immature.

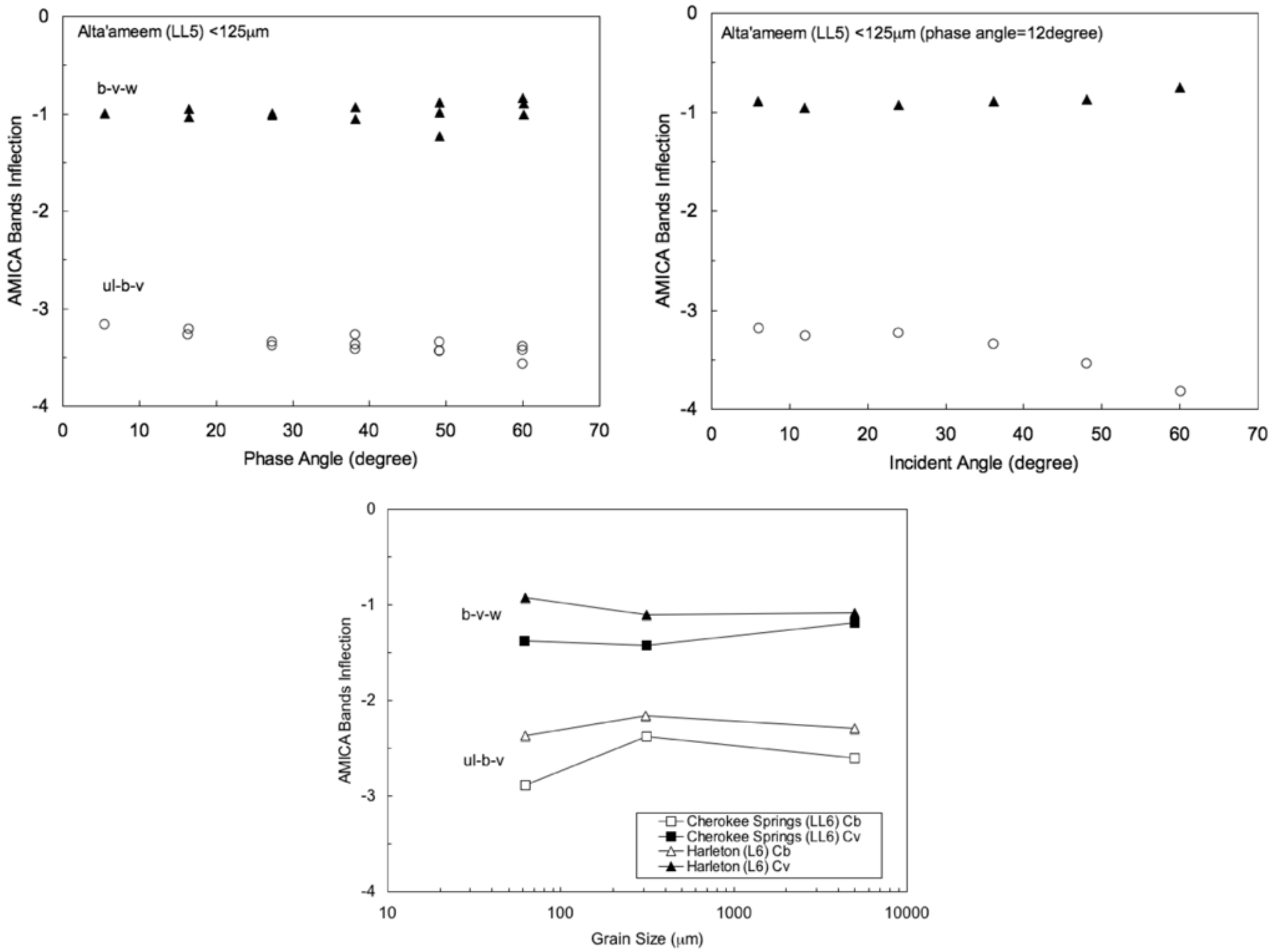

Fig. 6. Effects of viewing geometry and grain size on the amounts of ul-b-v-w inflections C_b and b-v-w inflection C_v. Effects of (a) phase angle and (b) incidence angle using an LL5 chondrite sample, and (c) the effect of grain size using LL6 chondrite chip and powder samples.

The circular area surrounding the Tanegashima boulders is reddish in R_w/R_b (Fig. 2b) and also dark red in the C_v index (Fig. 7b). This area may have a mature fine-material deposit. A similar trend is observed in Little Woomera Regio (Fig. 2c). There are, however, some regions that show unusual relationships between R_w/R_b and C_v. In Fig. 2d, MUSES-C Regio appears to gradually change from brighter and bluer on the western (Yatsugatake region) side to darker and redder on the eastern (boulder-rich) side on the R_w/R_b map. However, on the C_v map, MUSES-C Regio appears to be mostly space-weathered. The east-west variation in color and brightness of MUSES-C Regio may be caused by grain size, roughness of particles, or freshness change. Yano et al. (2006) reported that 1) MUSES-C Regio is filled with size-sorted regolith, mostly ranging from millimeter to centimeter scales; 2) no spectral variations in MUSES-C Regio were found by XRS or NIRS; and 3) MUSES-C Regio has the minimum potential over the entire surface of Itokawa. Their results suggest that particle segregation from the eastern side to Yatsugatake side (Yano et al. 2006; Miyamoto et al. 2007) may be explained by the color variation in Fig. 2d. In the case of freshness change, the change may be too subtle to detect using the C_v index. In all cases, it can be said that samples collected at touchdown probably include weathered surface materials, as the C_v map shows that the whole surface of MUSES-C Regio is weathered. Yoshinodai boulder looks fresh in both R_w/R_b and C_v maps. Half-buried boulders Tanegashima and Pencil look neutral or redder in the R_w/R_b map, but they are less matured in the C_v map. The accumulation process of rubble-pile asteroid might cause the immaturity of half-buried big boulders. Larger boulders, which formed the core of the asteroid in the early stage of the formation, were embedded in a blanket of smaller boulders (Britt and Consolmagno 2001), and have recently come to the surface due to external forces (e.g., seismic shaking or tidal force by planetary encounter). Another possibility is that a spallation of boulders on the surface could cause the freshness changes (Nakamura et al., Forthcoming). In this case, freshness heterogeneity on boulders can be expected. Further analysis using higher resolution color maps are needed.

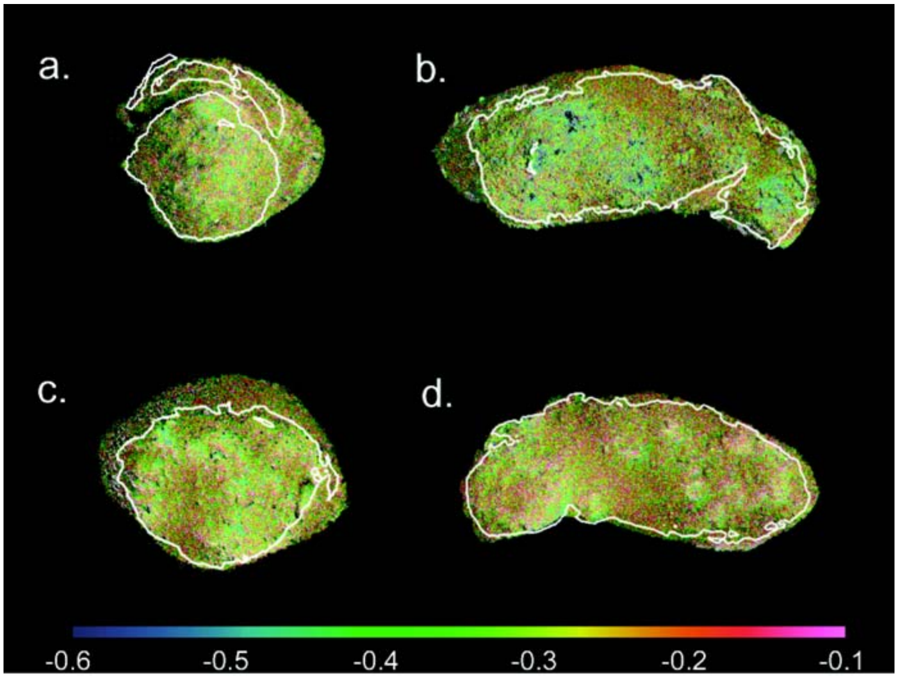

Fig. 7. Space-weathering index (C_v, b-v-w inflection) map overlaying a w-band image. The solid line denotes the boundary of the incident angle of 60°; at less than this angle, the index accurately shows the degree of space weathering.

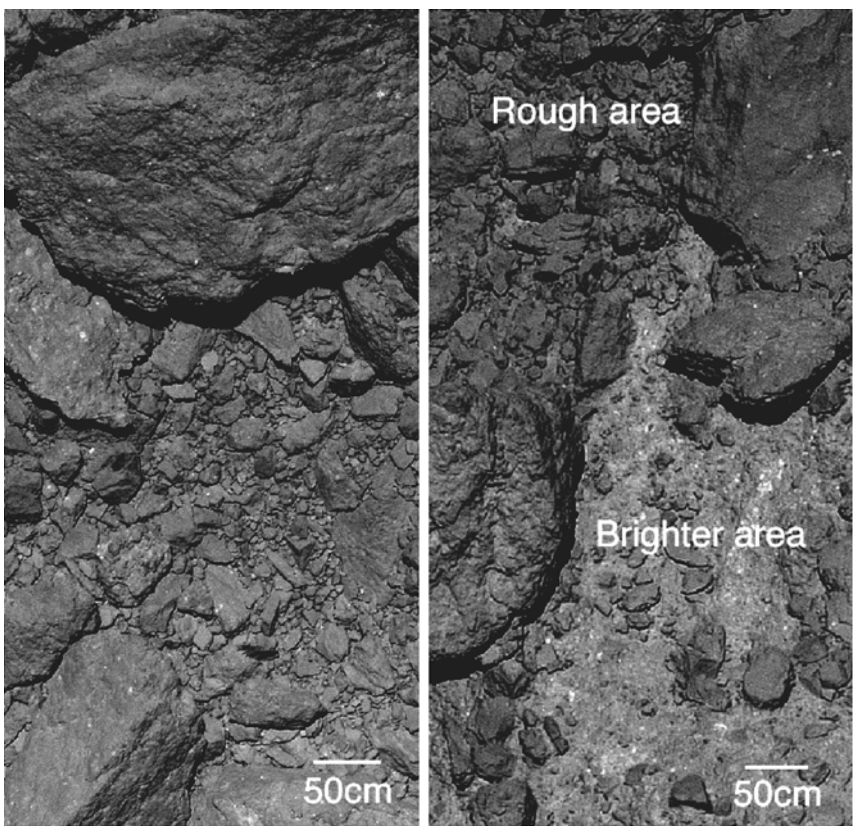

Fig. 8. Close-up images on the western side. Original lossless data were processed with the Lucy-Richardson image deconvolution algorithm in order to restore the blurred images. The spatial resolutions are 6 mm/pixel (left) and 9 mm/pixel (right). The left image (ST_2544579522) is of a ubiquitously rough area. The right image (ST_2544617921) is the boundary between a rough (boulder-rich) area and a brighter (fresher) area on the rim of LINEAR crater.

Comparison with Close-Up Monochromatic Images

In Fig. 8, we show high-resolution images of Itokawa rough terrains. These images were obtained during a touchdown rehearsal on November 12, 2005, using a v-band filter. Due to the Fourier image deconvolution process, the spatial resolutions of these two images are improved to the pixel resolutions, that is, 6 mm (Fig. 8a) and 9 mm (Fig. 8b). The left image (Fig. 8a) reveals that particles less than a centimeter in size are very limited, or even lacking, on the surface of this boulder-rich area. If the boulders are coated by finer particles, brightness heterogeneity caused by inhomogeneous thickness can be expected. Uniform darkness (the brightness difference is less than 10%) of the boulders and evidence of weathering in most boulder-rich terrain (e.g., rough terrain on the eastern side) suggests that the rocky surfaces are likely weathered in spite of the inefficiency of the processes there (Sasaki et al. 2006; Strazzulla et al. 2005). In close-up images, most bright (fresh) areas are observed to underlie dark boulders (Fig. 8b). This indicates that the brighter areas might reflect the subterranean fresh materials, which were exposed due to the removal of weathered boulders. While fresh material in craters can be explained by the excavation of the weathered layer by impact, freshness on steep slopes remains an open question. The lack of flow front and talus structure in Shirakami region cannot simply be explained by the removal of the superposed boulders (Saito et al. 2006). The existence of bright spots (Fig. 8a) and scars, which were probably produced by interplanetary dust particle bombardments, on dark boulders might support the assumption that the boulders on Itokawa are covered by thin weathered layers.

SUMMARY AND DISCUSSION

In this paper, we show the color images of the near-Earth asteroid Itokawa taken by Hayabusa's multi-band imaging camera AMICA. The disk-resolved measurements show large variations in three visible channels. We present a map of an index related to the degree of space weathering, and find large variations in the degree of space weathering on Itokawa. Unlike the large asteroids (>10 km) studied by previous space missions, this small asteroid has little or no regolith blanket. Instead, most of the surface of Itokawa is covered by weathered rocks and gravel, which require considerable time to develop weathered layers. In fact, the space-weathering index obtained from ECAS Version 3.0 shows that the surfaces of Ida ($C_v = 0.09 \pm 0.11$) and Gaspra ($C_v = -0.38 \pm 0.30$) would be more mature than that of Itokawa (disk-averaged $C_v = -0.49 \pm 0.02$).

Recent ground-based observations suggest that a color transition exists between ordinary chondrite-like objects and S-type asteroids over size range of 0.1–5 km, which implies that the surfaces of small asteroids are evolving toward the colors of larger asteroids (Binzel et al. 2004). The evidence arguing for less space weathering on small near-Earth asteroids obtained by ground-based observations implies that 1) these asteroids are young because collisions that generate new objects or fresh surfaces become much more frequent at small sizes (Bottke et al. 2005; O'Brien and Greenberg 2005), and 2) they do not have sufficient gravity to have a regolith blanket, which is susceptible to space weathering.

Acknowledgments–We would like to thank all members of the Hayabusa mission team for their support of the data acquisition. We thank Dr. Tsuko Nakamura and Ms. Masayo Nagano for their technical backup of the development and calibration of AMICA, and Prof. Makoto Yoshikawa for the useful discussion. We also thank Prof. Edward Cloutis and Dr. Sarah Noble for their critical reading of the manuscript and their helpful comments. Ranging data was given by the Hayabusa/LIDAR science group. Ground-based observations of Itokawa were supported by the Institute for Astronomy (IfA) at the University of Hawai'i. Samples of Harlton (USNM 7146), Cherokee Springs (USNM 1319), and Alta'ameem (USNM 5964) meteorites were loaned from the National Museum of Natural History, Smithsonian Institution. We thank Dr. Tim McCoy for his assistance. RELAB is a multi-user facility operated under NASA Planetary Geology and Geophysics Program.

Editorial Handling—Dr. Carlé Pieters

REFERENCES

Abe M., Takagi Y., Kitazato K., Abe S., Hiroi T., Vilas F., Clark B. E., Abell P. A., Lederer S., Jarvis K. S., Nimura T., Ueda Y., and Fujiwara A. 2006a. Near-infrared spectral results of asteroid Itokawa from the Hayabusa spacecraft. *Science* 312:1334–1338.

Abe S., Mukai T., Hirata N., Barnouin-Jha O., Cheng A. F., Demura H., Gaskell R. W., Hashimoto T., Hiraoka K., Honda T., Kubota T., Matsuoka M., Mizuno T., Nakamura R., Scheeres D. J., and Yoshikawa M. 2006b. Mass and local topography measurements of Itokawa by Hayabusa. *Science* 312:1344–1347.

Binzel R. P., Rivkin A. S., Bus S. J., Sunshine J. M., and Burbine T. H. 2001. MUSES-C target asteroid (25143) 1998 SF36: A reddened ordinary chondrite. *Meteoritics & Planetary Science* 36:1167–1172.

Binzel R. P., Rivkin A. S., Stuart J. S., Harris A. W., Bus S. J., and Burbine T. H. 2004. Observed spectral properties of near-Earth objects: Results for population distribution, source regions, and space weathering processes. *Icarus* 170:259–294.

Bottke W. F., Durda D. D., Nesvorný D., Jedicke R., Morbidelli A., Vokrouhlický D., and Levison H. F. 2005. Linking the collisional history of the main asteroid belt to its dynamical excitation and depletion. *Icarus* 179:63–94.

Britt D. T. and Consolmagno G. J. 2001. Modeling the structure of high-porosity asteroids. *Icarus* 152:134–139.

Cellino A., Yoshida F., Anderlucci E., Bendjoya P., Philippe di M., Ishiguro M., Nakamura A. M., and Saito J. 2005. A polarimetric study of asteroid 25143 Itokawa. *Icarus* 179:297–303.

Chapman C. R. 1996. S-type asteroids, ordinary chondrites, and space weathering: The evidence from Galileo's fly-bys of Gaspra and Ida. *Meteoritics & Planetary Science* 31:699–725.

Chapman C. R., Merline W. J., Thomas P. C., Joseph J., Cheng A. F., and Izenberg N. 2002. Impact history of Eros: Craters and boulders. *Icarus* 155:104–118.

Clark B. E., Lucey P., Helfenstein P., Bell J. F., Peterson C., Veverka J., McConnochie T., Robinson M. S., Bussey B., Murchie S. L., Izenberg N. I., and Chapman C. R. 2001. Space weathering on Eros: Constraints from albedo and spectral measurements of Psyche crater. *Meteoritics & Planetary Science* 36:1617–1637.

Demura H., Kobayashi S., Nemoto E., Matsumoto N., Furuya M., Yukishita A., Muranaka N., Morita H., Shirakawa K., Maruya M., Ohyama H., Uo M., Kubota T., Hashimoto T., Kawaguchi J., Fujiwara A., Saito J., Sasaki S., Miyamoto H., and Hirata N. 2006. Pole and global shape of 25143 Itokawa. *Science* 312:1347–1349.

Dermawan B., Nakamura T., Fukushima H., Sato H., Yoshida F., and Sato Y. 2002. CD photometry of the MUSES-C mission target: Asteroid 25143 1998 SF36. *Publications of the Astronomical Society of Japan* 54:635–640.

Fujiwara A., Kawaguchi J., Yeomans D. K., Abe M., Mukai T., Okada T., Saito J., Yano H., Yoshikawa M., Scheeres D. J., Barnouin-Jha O., Cheng A. F., Demura H., Gaskell R. W., Hirata N., Ikeda H., Kominato T., Miyamoto H., Nakamura A. M., Nakamura R., Sasaki S., and Uesugi K. 2006. The rubble-pile asteroid Itokawa as observed by Hayabusa. *Science* 312: 1330–1334.

Gaskell R., Saito J., Ishiguro M., Kubota T., Hashimoto T., Hirata N., Abe S., Barnouin-Jha O. S., and Scheeres D. 2006. Global topography of asteroid 25143 Itokawa (abstract #1876). 37th Lunar and Planetary Science Conference. CD-ROM.

Helfenstein P., Veverka J., Thomas P. C., Simonelli D. P., Lee P., Klaasen K., Johnson T. V., Breneman H., Head J. W., and Murchie S. 1994. Galileo photometry of asteroid 951 Gaspra. *Icarus* 107:37–60.

Hiroi T. and Pieters C. M. 1994. Estimation of grain sizes and mixing ratios of fine powder mixtures of common geologic minerals. *Journal of Geophysical Research* 99:10,867–10,879.

Hiroi T., Ueda Y., Nimura T., Abe M., Ishiguro M., and Sasaki S. 2006a. A new scheme for estimating the degree of space weathering through visible multiband spectroscopy using an ECAS-type filter system such as Hayabusa AMICA (abstract #1396). 37th Lunar and Planetary Science Conference. CD-ROM.

Hiroi T., Abe M., Kitazato K., Abe S., Clark B. E., Sasaki S., Ishiguro M., and Barnouin-Jha O. 2006b. Developing space weathering on the asteroid 25143 Itokawa. *Nature* 443:56–58

Ishiguro M., Abe M., Ohba Y., Fujiwara A., Fuse T., Terada H., Goto M., Kobayashi N., Tokunaga A. T., and Hasegawa S. 2003. Near-infrared observations of MUSES-C mission target. *Publications of the Astronomical Society of Japan* 55:691–699.

Kaasalainen M., Kwiatkowski T., Abe M., Piironen J., Nakamura T., Ohba Y., Dermawan B., Farnham T., Colas F., Lowry S., Weissman P., Whiteley R. J., Tholen D. J., Larson S. M., Yoshikawa M., Toth I., and Velichko F. P. 2003. CCD photometry and model of MUSES-C target (25143) 1998 SF36. *Astronomy and Astrophysics* 405:L2–L32.

Lederer S. M., Domingue D. L., Vilas F., Abe M., Farnham T. L., Jarvis K. S., Lowry S. C., Ohba Y., Weissman P. R., French L. M., Fukai H., Hasegawa S., Ishiguro M., Larson S. M., and Takagi Y. 2005. Physical characteristics of Hayabusa target asteroid 25143 Itokawa. *Icarus* 173:153–165.

Lowry S. C., Weissman P. R., Hicks M. D., Whiteley R. J., and Larson S. 2005. Physical properties of asteroid (25143) Itokawa—Target of the Hayabusa sample return mission. *Icarus* 176:408–417.

Lucy L. B. 1974. An iterative technique for the rectification of observed distributions. *The Astronomical Journal* 79:745–754.

Miyamoto H., Yano H., Scheeres D. J., Abe S., Barnouin-Jha O., Cheng A. F., Demura H., Gaskell R. W., Hirata N., Ishiguro M., Michikami T., Nakamura A. M., Nakamura R., Saito J., and Sasaki S. 2007. Regolith migration and sorting on asteroid Itokawa. *Science* 316:1011–1014.

Müller T. G., Sekiguchi T., Kaasalainen M., Abe M., and Hasegawa S. 2005. Thermal infrared observations of the Hayabusa spacecraft target asteroid 25143 Itokawa. *Astronomy and Astrophysics* 443:347–355.

Murchie S., Robinson M., Clark B., Li H., Thomas P., Joseph J., Bussey B., Domingue D., Veverka J., Izenberg N., and Chapman C. 2002. Color variations on Eros from NEAR multispectral imaging. *Icarus* 155:145–168.

Nakamura A. M., Michikami T., Hirata N., Fujiwara A., Nakamura R., Ishiguro M., Miyamoto H., Demura H., Hiraoka K., Honda T., Honda C., Saito J., Hashimoto T., and Kubota T. Forthcoming. Impact process of boulders on the surface of asteroid 25143 Itokawa: Fragments from collisional disruption. *Earth, Planets, and Space.*

Nakamura T., Nakamura A. M., Saito J., Sasaki S., Nakamura R., Demura H., Akiyama H., Tholen D., and the AMICA team. 2001. Multi-band imaging camera and its sciences for the Japanese near-Earth asteroid mission MUSES-C. *Earth, Planets and Space* 53:1047–1063.

O'Brien D. P. and Greenberg R. 2005. The collisional and dynamical evolution of the main-belt and NEA size distributions. *Icarus* 178:179–212.

Ohba Y., Abe M., Hasegawa S., Ishiguro M., Kwiatkowski T., Colas F., Dermawan B., and Fujiwara A. 2003. Pole orientation and triaxial ellipsoid shape of (25143) 1998 SF36, a target asteroid of the MUSES-C mission. *Earth, Planets and Space* 55: 341–347.

Okada T., Shirai K., Yamamoto Y., Arai T., Ogawa K., Hosono K., and Kato M. 2006. X-ray fluorescence spectrometry of asteroid Itokawa by Hayabusa. *Science* 312:1338–1341.

Ostro S. J., Benner L. A. M., Nolan M. C., Magri C., Giorgini J. D., Scheeres D. J., Broschart S. B., Kaasalainen M., Vokrouhlický D., Chesley S. R., Margot J.-L., Jurgens R. F., Rose R., Yeomans D. K., Suzuku S., and de Jong E. M. 2004. Radar observations of asteroid 25143 Itokawa (1998 SF36). *Meteoritics & Planetary Science* 39:1167–1172.

Pieters C. M., Fischer E. M., Rode O., and Basu A. 1993. Optical effects of space weathering: The role of the finest fraction. *Journal of Geophysical Research* 98:20,817–20,824.

Richardson W. H. 1972. Bayesian-based iterative method of image restoration. *Journal of the Optical Society of America* 62:55–59.

Saito J., Miyamoto H., Nakamura R., Ishiguro M., Michikami T., Nakamura A. M., Demura H., Sasaki S., Hirata N., Honda C., Yamamoto A., Yokota Y., Fuse T., Yoshida F., Tholen D. J., Gaskell R. W., Hashimoto T., Kubota T., Higuchi Y., Nakamura T., Smith P., Hiraoka K., Honda T., Kobayashi S., Furuya M., Matsumoto N., Nemoto E., Yukishita A., Kitazato K., Dermawan B., Sogame A., Terazono J., Shinohara C., and Akiyama H. 2006. Detailed images of asteroid 25143 Itokawa from Hayabusa. *Science* 312:1341–1344.

Sakai T. and Nakamura A. M. 2005. Quantification of porosity and surface roughness in laboratory measurements of the bidirectional reflectance of asteroid surface analogues. *Earth, Planets and Space* 57:71–76.

Sasaki S., Nakamura K., Hamabe Y., Kurahashi E., and Hiroi T. 2001. Production of iron nanoparticles by laser irradiation in a simulation of lunar-like space weathering. *Nature* 410:555–557.

Sasaki S., Nimura T., Hiroi T., Ishiguro M., Hirata N., Abe M., Ueda Y., Yamamoto A., and Clark B. E. 2006. Space weathering of rock surface without regolith: Laboratory simulation of spectral change (abstract #1705). 37th Lunar and Planetary Science Conference. CD-ROM.

Sekiguchi T., Abe M., Boehnhardt H., Dermawan B., Hainaut O. R., and Hasegawa S. 2003. Thermal observations of MUSES-C mission target (25143) 1998 SF36. *Astronomy and Astrophysics* 397:325–328.

Strazzulla G., Dotto E., Binzel R., Brunetto R., Barucci M. A., Blanco A., and Orofino V. 2005, Spectral alteration of the meteorite Epinal (H5) induced by heavy ion irradiation: A simulation of space weathering effects on near-Earth asteroids. *Icarus* 174:31–35.

Tedesco E. F., Tholen D. J., and Zellner B. 1982. The eight-color asteroid survey—Standard stars. *The Astronomical Journal* 87: 1585–1592.

Veverka J., Helfenstein P., Lee P., Thomas P., McEwen A., Belton M., Klaasen K., Johnson T. V., Granahan J., Fanale F., Geissler P., and Head J. W. 1996. Ida and Dactyl: Spectral reflectance and color variations. *Icarus* 120:66–76.

Yano H., Kubota T., Miyamoto H., Okada T., Scheeres D., Takagi Y., Yoshida K., Abe M., Abe S., Barnouin-Jha O., Fujiwara A., Hasegawa S., Hashimoto T., Ishiguro M., Kato M., Kawaguchi J., Mukai T., Saito J., Sasaki S., and Yoshikawa M. 2006. Touchdown of the Hayabusa spacecraft at the Muses Sea on Itokawa. *Science* 312:1350–1353.

Zellner B., Tholen D. J., and Tedesco E. F. 1985. The eight-color asteroid survey—Results for 589 minor planets. *Icarus* 61:355–416.